Available online at www.sciencedirect.com
SCIENCE DIRECT
Journal of Molecular Catalysis A: Chemical 251 (2006) 263–269
JOURNAL OF MOLECULAR CATALYSIS A: CHEMICAL
www.elsevier.com/locate/molcata

Synthesis, spectroscopy, and structures of chiral rhodium(I) corrole complexes

Irena Saltsman [a], Yael Balazs [a], Israel Goldberg [b,**], Zeev Gross [a,*]

[a] *Department of Chemistry and Institute of Catalysis Science and Technology, Technion-Israel Institute of Technology, Haifa 32000, Israel*
[b] *School of Chemistry, Tel Aviv University, Tel Aviv 69978, Israel*

Available online 20 March 2006

Abstract

The easily accessible chiral corrole **1** was metallated by rhodium and isolated with additional ligands of very different electronic and steric properties: two carbonyls, a cyclic diphosphine, and a diene. The diamagnetic rhodium(I) complexes were characterized by multinuclear NMR methods and X-ray crystallography. The diphosphine-coordinated complex **2b** was obtained non-racemic, which was further confirmed by circular dichroism.

Keywords: Rhodium complexes; Corroles; X-ray crystallography

1. Introduction

The recently introduced synthetic methodologies for facile preparation of triarylcorroles [1], coordination-core contracted analogs of tetraarylporphyrins, allowed for the utilization of the corresponding metal complexes as catalysts for various transformations [2,3]. These include hydroxylation of alkanes [2] and epoxidation [4], aziridination [5], and cyclopropanation [6] of alkenes. Triphenylphosphine-coordinated rhodium(III) corroles were shown to be potent catalysts for carbene-transfer from ethyl diazoacetate (EDA) to olefins [6] and several such complexes were fully characterized by NMR and X-ray crystallography [6,7]. The present investigations focus on the recently introduced chiral corrole **1** (Scheme 1) [8] as the first step toward catalysis by chiral corrole metal complexes. We report the syntheses of several rhodium(I) complexes of **1** that differ significantly in the steric and electronic features of the other metal-coordinated ligands. All complexes were fully characterized by multinuclear NMR methods and X-ray crystallography.

* Corresponding author. Fax: +972 4 829 5703.
** Corresponding author. Fax: +972 3 640 9293.
E-mail addresses: goldberg@chemsg7.tau.ac.il (I. Goldberg), chr10zg@tx.technion.ac.il (Z. Gross).

1381-1169/$ – see front matter © 2006 Elsevier B.V. All rights reserved.
doi:10.1016/j.molcata.2006.02.030

2. Experimental

2.1. Physical methods

NMR spectra were recorded at room temperature on a Bruker Avance 300 spectrometer (AV300) equipped with a QNP 1H/19F/31P/13C-2H 5 mm probehead (operating at 300 MHz for ^{1}H and 282 MHz for ^{19}F) or on a Bruker Avance 500 spectrometer (AV500) equipped with a bbo probehead (operating at 500 MHz for ^{1}H, 202 MHz for ^{31}P, and 125 MHz for ^{13}C). Chemical shifts are reported in ppm relative to solvent signals ($\delta_H = 7.15$ and $\delta_C = 128.0$ for benzene-d_6 or $\delta_H = 7.24$ and $\delta_C = 77.0$ for chloroform-*d*) or relative to $CFCl_3$ ($\delta_F = 0.00$). Coupling constants (*J*) are reported in Hz.

The ^{19}F-decoupled ^{1}H-observed NMR spectra were recorded on the AV300 using the zghfigqn pulse program (XWIN-NMR Version 3.1) and waltz16 composite pulse decoupling. Control experiments were run with full attenuation (120 dB) on the ^{19}F pulses, but otherwise identical conditions. ^{31}P-decoupling of ^{1}H-observed NMR spectra was achieved with cw irradiation on the AV500 using the zgcw pulprogram (45 dB attenuation of the X-amplifier or 120 dB attenuation in control experiments).

^{13}C NMR spectra were acquired with inverse-gated ^{1}H decoupling on the AV500; a total of 20,480 transients were

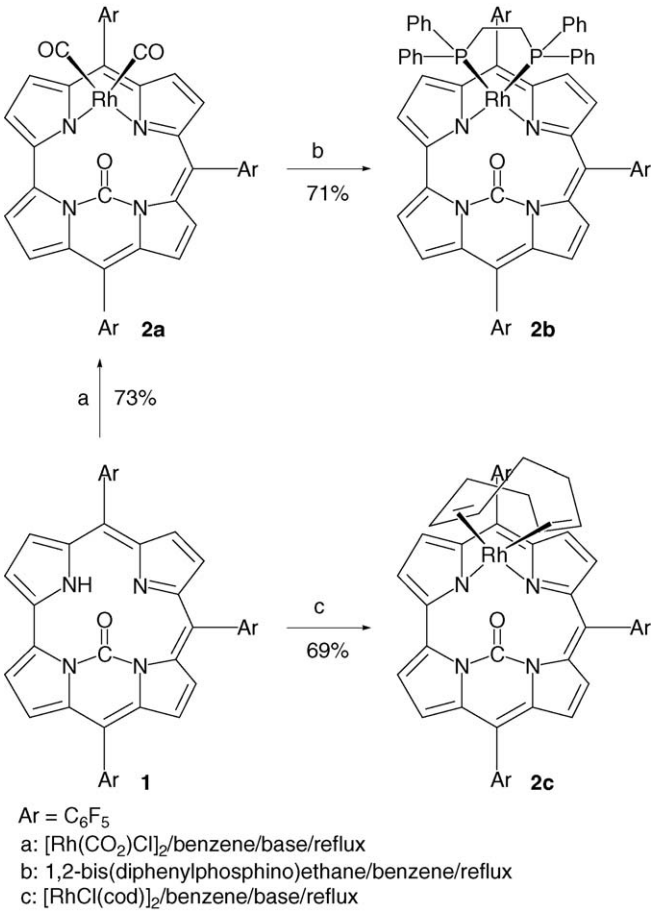

Scheme 1.

collected using a 6 s repetition delay. To distinguish between two doublet peaks and a single dd peak, spectra were recorded at two different fields.

A HP 8452A diode array spectrophotometer was used to record the electronic spectra. Mass spectroscopy was performed on a Finnigan TSQ 70 instrument with isobutene as carrier gas. The diffraction measurements were carried out on a Nonius Kappa CCD diffractometer, using graphite monochromated Mo Kα radiation (λ = 0.7107 Å).

2.2. Materials

All reagents were purchased from commercial sources and used as received unless otherwise noted. Benzene (Merck, thiophene-free) was dried over calcium hydride and distilled. $[Rh_2(CO)_4Cl_2]$ (Strem) and $[Rh(cod)Cl]_2$ (cod = 1,5-cyclooctadiene) (Aldrich) were used as received.

2.3. Synthetic methods

The synthetic details for the preparation of the chiral N^{21},N^{22}-carbamide-5,10,15-tris(pentafluorophenyl)corrole (**1**) and its precursor 5,10,15-tris(pentafluorophenyl)corrole H_3 (tpfc) are provided in previous publications [8,9].

2.4. Insertion of Rh(I)

2.4.1. Preparation of the bis-(carbonmonoxide)rhodium(I) complex of *1*, *2a*

The preparation of **2a** and its physical properties are described in a previous publication [10]. X-ray quality crystals of **2a** were obtained in the current studies via recrystallization from benzene and *n*-heptane.

2.4.2. Preparation of the (1,2-bis-(diphenylphosphino)ethane)rhodium(I) complex of *1*, *2b*

1,2-Bis-(diphenylphosphino)ethane (DIPHOS) (0.29 g, 0.73 mmol) was added to a solution of **2a** (0.06 g, 0.073 mmol) in dry benzene (10 mL). The mixture was refluxed overnight, after which the color changed from green-red to dark-green and TLC examination revealed no starting material. Solvent evaporation and carefully separation by chromatographic column of the residue (silica gel, 5% ethyl acetate in *n*-hexane) afforded **2b** as dark-green solid (0.058 g, 71% yield). X-ray quality crystals obtained by recrystallization from THF and *n*-heptane. The obtained crystals found to be non-racemic by X-ray crystallography and circular dichroism.

R_f (silica, *n*-hexane:ethyl acetate, 5:1) = 0.54.

^{1}H NMR (C_6D_6, $\delta = 7.15$): $\delta = 8.31$ (d, ^3J(H,H) = 4.5 Hz, 1H), 8.02 (d, ^3J(H,H) = 5.1 Hz, 1H), 7.92 (d, ^3J(H,H) = 5.1 Hz, 1H), 7.77 (d, ^3J(H,H) = 4.5 Hz, 1H), 7.64 (d, ^3J(H,H) = 4.2 Hz, 1H), 7.59 (d, ^3J(H,H) = 4.5 Hz, 1H), 7.54 (m, 1H), 7.31 (d, ^3J(H,H) = 4.5 Hz, 1H), 6.78–6.63 (m, 8H), 5.47 (t, ^3J(H,H) = 7.8 Hz, 2H), 5.28 (t, ^3J(H,H) = 8.4 Hz, 2H), 1.30–1.16 (m, 8H), 1.11 (t, ^3J(H,H) = 4.2 Hz, 4H).

^{19}F NMR (C_6D_6): $\delta = -135.22$ (d, ^3J(F,F) = 24.6 Hz, 1F), −136.93 (d, ^3J(F,F) = 23.2 Hz, 1F), −137,40 (d, ^3J(F,F) = 24.0 Hz, 2F), −138.64 (d, ^3J(F,F) = 24.0 Hz, 1F), −139.57 (d, ^3J(F,F) = 24.6 Hz, 1F), −152.03 (t, ^3J(F,F) = 22.9 Hz, 1F), −152.81 (t, ^3J(F,F) = 21.5 Hz, 1F), −153.58 (t, ^3J(F,F) = 22.0 Hz, 1F), −160.41 (t, ^3J(F,F) = 23.7 HZ, 1F), −161.82 (t, ^3J(F,F) = 24.0 Hz, 1F), −162.64 (m, 2F), −163.78 (m, 2F).

^{31}P NMR (C_6D_6): $\delta = 66.3$ (dd, ^1J(Rh,P_1) = 179 Hz, Rh–P_1, ^2J(P_1,P_2) = 44 Hz, P_1–P_2), 60.17 (dd, ^1J(Rh,P_2) = 179 Hz, Rh–P_2, ^2J(P_2,P_1) = 44 Hz, P_2–P_1).

UV–vis (EtOAc): λ_{max} 409 nm (ε 92,000), 590 nm (21,000).

MS (MALDI-TOF): *m*/*z* (%): 1322.3 [M^+, 100%].

2.5. Preparation of the (1,5-cyclooctadiene)rhodium(I) complex of *1*, *2c*

The lithium salt of hexamethyldisilazane (0.059 g, 0.35 mmol) was added to an Ar purged solution of **1** (0.029 g, 0.035 mmol) in dry benzene (10 mL) and the mixture was heated to reflux for 15 min, after which $[Rh(cod)Cl]_2$ (0.02 g, 0.04 mmol) was added in portions over 30 min. During reaction, the mixture turned from red to deep green and no starting material was present after heating to reflux overnight. The reaction mixture was cooled to RT and washed with water two times, extracted with dichloromethane, dried by anhydrous sodium sulfate, filtered, and evaporated to dryness.

Flash column chromatography (silica gel, 1% ethyl acetate in *n*-hexane) afforded **2c** as green solid (25 mg; 69% yield). X-ray quality crystals obtained by recrystallization from benzene and *n*-heptane.

R_f (silica, *n*-hexane: ethyl acetate, 4:1) = 0.62.

^{1}H NMR (C_6D_6, $\delta = 7.15$): $\delta = 8.86$ (d, ^3J(H,H) = 4.5 Hz, 1H), 8.38 (d, ^3J(H,H) = 5.1 Hz, 1H), 8.25 (d, ^3J(H,H) = 5.1 Hz, 1H), 8.02–7.97 (m, 3H), 7.95 (d, ^3J(H,H) = 4.5 Hz, 1H), 7.53 (d, ^3J(H,H) = 4.5 Hz, 1H), 0.15–0.13 (m, 4H), −0.14 (m, 2H), −0.15 (br s, 1H), −0.32 (m, 2H), −0.89 (m, 2H), −1.47 (br s, 1H).

^{19}F NMR (C_6D_6): $\delta = -136.23$ (d, ^3J(F,F) = 22.3 Hz, 1F), −137.67 (d, ^3J(F,F) = 24.2 Hz, 1F), −138.39 (d, ^3J(F,F) = 24.0 Hz, 1F), −138.90 (m, 2F), −139.36 (d, ^3J(F,F) = 23.4 Hz, 1F), −152.04 (q, ^3J(F,F) = 20.8 Hz, 2F), −152.85 (t, ^3J(F,F) = 21.2 Hz, 1F), −160.81 (dd, ^3J(F,F) = 23.7 Hz, ^4J(F,F) = 6.8 Hz, 2F), −161.78 (dd, ^3J(F,F) = 22.6 Hz, ^4J(F,F) = 7.3 Hz, 2F), −162.73 (dd, ^3J(F,F) = 21.4 Hz, ^4J(F,F) = 6.5 Hz, 2F).

UV–vis (EtOAc): λ_{max} 385 nm (ε 66,000), 408 nm (82,000), 584 nm (20,000).

MS (MALDI-TOF): *m*/*z* (%): 1031.8 [M^+, 100%].

2.6. X-ray crystallography

The diffraction measurements were carried out on a Nonius Kappa CCD diffractometer, using graphite monochromated Mo Kα radiation (λ = 0.7107 Å). The crystalline samples of the analyzed compounds were covered with a thin layer of light oil and freeze-cooled to ca. 110 K in order to minimize solvent escape, structural disorder and thermal motion effects, and increase the precision of the results. The crystal structures were solved by direct and Patterson methods (SIR-92/97, DIRDIF-96) [11,12], and refined by full-matrix least squares on F^2 (SHELXL-97) [13]. All non-hydrogen atoms were refined anisotropically. Most of the hydrogen atoms (excluding those of the severely disordered solvent) were located in idealized positions, and were refined using a riding model, with $U_{iso} = 1.2$ or $1.5U_{eq}$ of the parent atom. The crystal and experimental data for all the compounds are summarized in Table 1.

All three complexes crystallized as solvates with either *n*-heptane (in **2a** and **2c**) or THF (**2b**). The corrole:solvent ratio is 1:1 in **2a**, 1:2 1/2 in **2b** and 1:2 in **2c**. The lattice-included molecules of these solvents reveal considerable disorder even at ca. 110 K and could not be modeled with high precision. Correspondingly, the highest residual electron-density peaks and troughs (∼1.0–1.1 e Å^{-3}) were found near the disordered solvent species. The crystals of the three materials diffract rather poorly, and the crystallographic refinements concluded in relatively high values. In all cases, however, they resulted in reliable structural models of the corrole complexes. The asymmetric unit of **2c** consists of two corrole units. Two out of the three compounds, **2a** and **2c**, crystallized as racemic mixtures in centrosymmetric crystals. Spontaneous resolution of the inherently chiral compound occurred only in the case of **2b**, which crystallized in a non-centric polar space group $P2_1$.

Table 1
Crystal data and experimental parameters of the structural analyses

Compound[a]	**2a**	**2b**	**2c**
Formula weight	1080.61	1503.05	1232.97
Crystal system	Monoclinic	Monoclinic	Triclinic
Space group	$P2_1/c$	$P2_1$	$P\bar{1}$
T (°C)	−163(2)	−163(2)	−163(2)
a (Å)	20.0347(5)	14.8502(6)	9.1884(3)
b (Å)	29.1808(9)	13.5533(3)	16.5431(6)
c (Å)	14.5672(6)	16.9828(6)	19.4446(7)
α (°)	90.0	90.0	113.024(2)
β (°)	100.140(2)	102.790(1)	102.711(2)
γ (°)	90.0	90.0	91.100(2)
V (Å^3)	8383.4(5)	3333.3(2)	2635.2(2)
Z	8	2	2
μ(Mo Kα) (mm^{-1})	0.52	0.40	0.42
ρ_{calcd} (g cm^{-3})	1.712	1.498	1.554
Data collected	31901	27836	21326
Unique reflections	11571	11426	11273
R_{int}	0.098	0.088	0.031
Data with $I > 2\sigma$	6881	10165	9180
Refined parameters	1165	865	738
R ($I > 2\sigma$)	0.076	0.063	0.052
R (all data)	0.146	0.073	0.068
R_w ($I > 2\sigma$)	0.129	0.137	0.129
R_w (all data)	0.155	0.142	0.141
$\lvert\Delta\rho\rvert_{max}$ (e Å^{-3})	0.63	1.02	1.12

[a] Chemical formulae: **2a**, $C_{40}H_8F_{15}N_4O_3Rh{\cdot}C_7H_{16}$; **2b**, $C_{64}H_{32}F_{15}N_4OP_2Rh{\cdot}2(1/2)C_4H_8O$; **2c**, $C_{46}H_{20}F_{15}N_4ORh{\cdot}2C_7H_{16}$.

3. Results and discussions

3.1. Synthesis

The synthetic methodologies for the preparation of the various rhodium complexes are summarized in Scheme 1. The common starting point is the chiral derivative **1**, obtained from the reaction of tris(pentafluorophenyl)corrole (readily accessible from solvent-free condensation of pyrrole and pentafluorobenzaldehyde) with phosgene [8,9]. The reaction of racemic **1** with $[Rh_2(CO)_4Cl_2]$ led to the rhodium(I) complex **2a**, whose coordination sphere consists of two nitrogen atoms from the corrole and two CO ligands. These conclusions were previously drawn from the NMR and IR spectra of **2a**, while the present investigation adds structural information that is based on X-ray crystallography. Earlier attempts of substituting the two reactivity-lowering carbonyl ligands by triphenylphosphine revealed that the reaction stopped (in 95% yield) after a single CO substitution [10]. The cyclic DIPHOS was employed in the current studies, anticipating that turning the second substitution into an intramolecular process would lead to the desired product. Indeed, complex **2b** was obtained in 69% isolated yield.

A direct route was applied for the synthesis of complex **2c**, by using $[Rh(cod)Cl]_2$ as the source for both the metal ion and the 1,5-cyclooctadiene (cod) ligand. The use of the strong base lithium hexamethyldisilazane for deprotonation of **1** in the non-polar benzene proved to be highly advantageous [7b]. The reaction proceeded quite well at relative low temperatures and short reaction times, with almost equimolar concentrations of corrole, base, and metal source.

3.2. NMR spectroscopy

The combination of ^{1}H, ^{13}C, ^{31}P, and ^{19}F NMR spectroscopy allowed for quite detailed structural information about the various complexes. First, the sharp signals indicated that all complexes are diamagnetic and thus indicative of rhodium(I) complexes, charge balanced by deprotonation of the single NH proton in **1** (Scheme 1). The ^{13}C NMR spectrum of complex **2a** (Fig. 1a) displays three types of carbonyl resonances, of which that at 153.8 ppm may safely be assigned to be the one bound to the corrole N atoms as it is a singlet that is also present in **1** (at 147.5 ppm). The two other carbonyls are assigned to be rhodium-coordinated by virtue of their Rh–CO coupling constants (179.5 ppm, d, ^{1}J(C,Rh) = 68.7 Hz and 179.1 ppm, d, ^{1}J(C,Rh) = 67.3 Hz) being in the range expected for rhodium carbonyls [14]. The data so far are consistent with the drawing of complex **2a** in Scheme 1: a square-planar rhodium(I) complex that is coordinated by two different carbonyls and two different N atoms, one neutral and one anionic. The absence of any symmetry element in **2a** (a "chiral metal" complex) should further be reflected by eight non-equivalent β-pyrrole CH protons and three sets (*ortho*, *meta*, *para*) of F atoms for each of the C_6F_5 rings in the ^{1}H and ^{19}F NMR spectra, respectively. However, both spectra were not at high enough resolution to confirm these expectations (Fig. 1b and c). Accordingly, and based on previous experience with tris(pentafluorophenyl)corrole, the ^{19}F-decoupled ^{1}H NMR spectrum of **2a** was obtained. This procedure resulted in the spectrum shown in Fig. 1d where the doublets due to β-pyrrole CH protons are more resolved.

The transformation of **2a** into the DIPHOS-coordinated rhodium(I) complex **2b** was reflected by a much more resolved ^{19}F spectrum and some changes in the ^{1}H chemical shifts of the eight non-equivalent β-pyrrole CH protons of the corrole (Fig. 2a and b). More significantly, the DIPHOS ligand was also clearly apparent: its phenyl protons appeared as two sets at relatively high field (<7 ppm), most easily seen for the *ortho*-H triplets at 5.47 and 5.28 ppm. The ^{31}P NMR spectrum of **2b** (Fig. 2c) further confirmed the asymmetric environment experienced by the ligand, reflected by an about 5 ppm difference in chemical shift and mutual coupling of the two P atoms (J = 44 Hz).

The ^{19}F and the low field ^{1}H NMR spectra of the COD-coordinated rhodium(I) complex **2c** (Fig. 3a and b) are quite similar to those of **2a** and **2b**, but the high field section of its ^{1}H NMR spectrum (Fig. 3, bottom) is distinctive. The resonances at <0 ppm may safely be assigned to the COD protons, experiencing a very large upfield shift (relative to non-

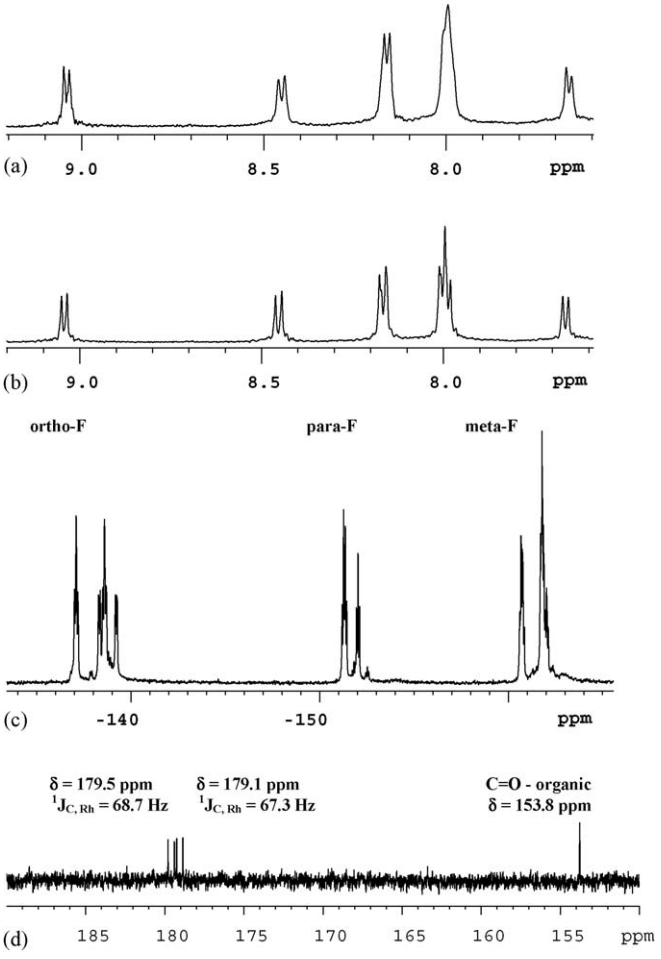

Fig. 1. NMR spectra of the biscarbonylrhodium(I) corrole **2a**: (a) ^{1}H, (b) ^{19}F-decoupled ^{1}H, (c) ^{19}F, and (d) ^{13}C.

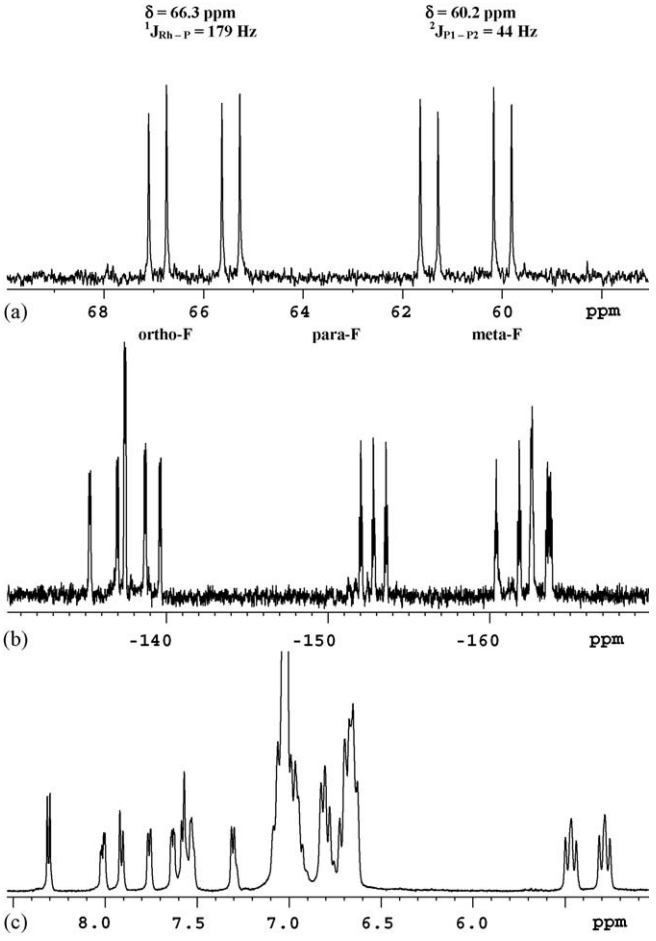

Fig. 2. NMR spectra of the DIPHOS-coordinated rhodium(I) complex **2b**: (a) ^{31}P, (b) ^{19}F, and (c) ^{1}H.

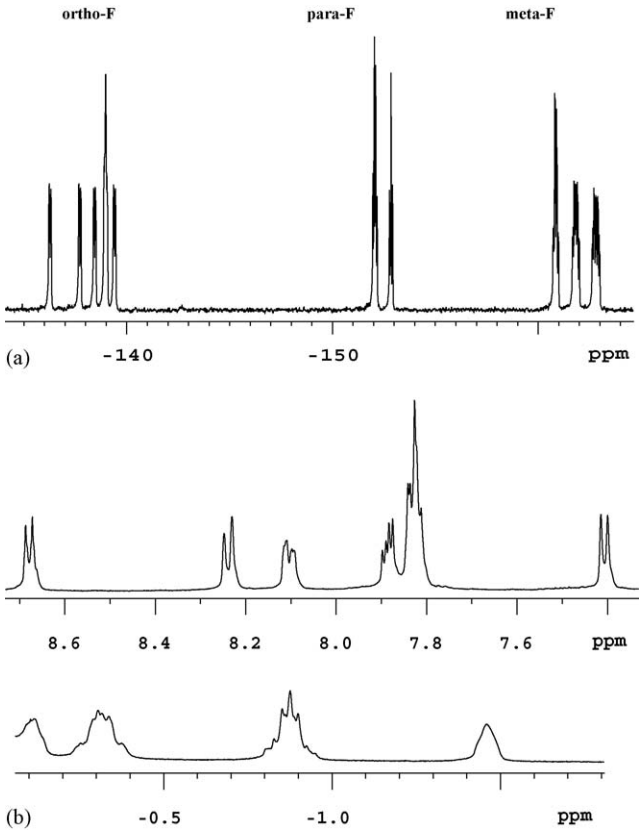

Fig. 3. ^{19}F (a) and ^{1}H (b) NMR spectra of the COD-coordinated rhodium(I) complex **2c**.

coordinated COD) due to the diamagnetic current effect of the corrole.

3.3. X-ray crystallography

The molecular plots of complexes **2a–c** are shown in Fig. 4. All the rhodium(I) complexes, obtained from the chiral ligand **1**, show a similar coordination mode. They represent severely crowded and geometrically distorted structures. The rhodium(I) ion perches on the corrole macrocycle from above, binding to two of the pyrrole nitrogen sites N_a and N_b that are not bridged by the organic carbonyl. Correspondingly, these pyrroles (labeled as 'a' and 'b') twist upwards in order to facilitate coordination to the metal ion. The common square-planar coordination environment of the rhodium is complemented by the apical ligands: two carbonyl groups in **2a**, the bidentate bis(diphenylphosphino)ethane moiety ligated to the metal via the P-sites in **2b**, and the bidentate cyclooctadiene residue that bind to the metal via the two double bonds in **2c**. In all cases the carbonyl bridged pyrrole rings (labeled 'b' and 'c') are nearly coplanar, the organic carbonyl itself being severely twisted downward due to the strain imposed on the corrole framework by, and to avoid collision with, the perching rhodium ion. Selected geometric parameters of the rhodium(I) corroles characterized in this study are listed in Table 2. They describe the twisted conformation of the corrole macrocycle, deviations in opposite directions of the carbonyl and the Rh-metal from the mean plane of the nearly co-planar pyrrole

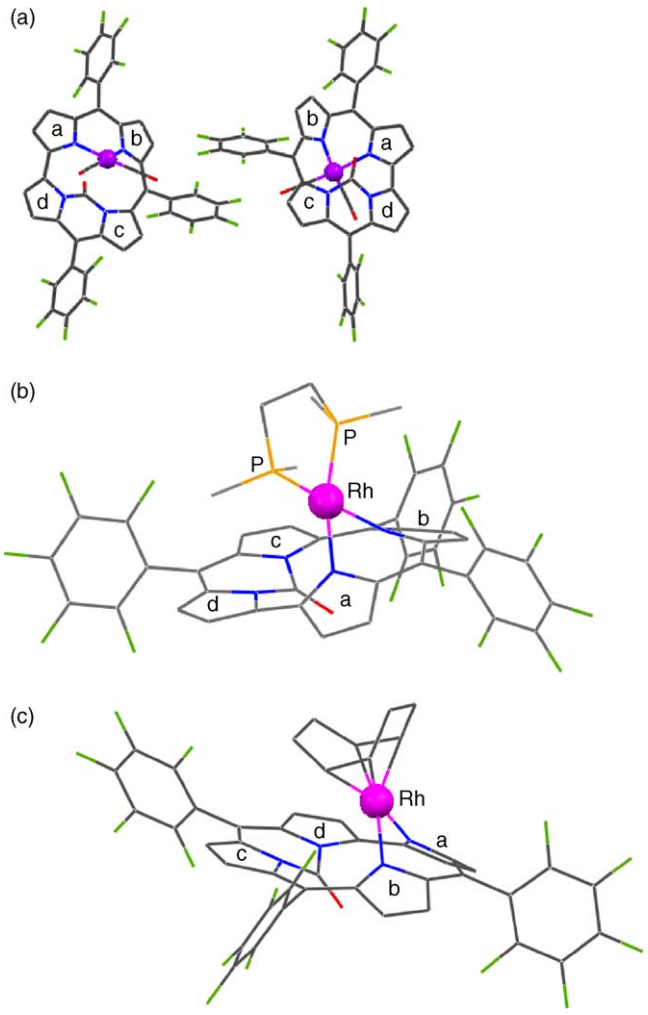

Fig. 4. Molecular structures of the corrole complexes (hydrogen atoms are omitted for clarity). The pyrrole rings are labeled consistently by 'a'–'c'. (a) The two crystallographically independent molecules in **2a**. (b) Structure of **2b**: the four phenyl rings bound to the P-atoms of the ligand are excluded. (c) Structure of **2c**. Note that the spontaneously resolved compound **2b** is represented by the observed enantiomer. The opposite isomers are shown for the racemic centrosymmetric crystal structures of **2a** and **2c**.

rings 'c' and 'd', and the coordination Rh–N, Rh–C(inorganic carbonyl), Rh–P, and Rh–C('cod') distances. The overall shape of these structures is also exhibited by dihedral angles between the mean plane defined by pyrrole rings 'c' and 'd' and that formed by Rh and the four sites coordinated to it, which involve atoms N_a, N_b, and two inorganic carbonyl C-atoms in **2a**, or two P-atoms in **2b**, or the midpoints of the two double bonds of the COD ligand in **2c**. These angles are 45.8(2) and 47.0(3)° in **2a**, 67.0(1)° in **2b**, and 55.4(2)° in **2c**. The crystal structures of **2a** and **2c** represent racemic compounds (space groups $P2_1/c$ and P-1). On the other hand, that of **2b** was obtained in a resolved form, crystallizing in a polar $P2_1$ space group. It is reasonable to assume that this different behavior could be effected by the bulkier bis-(diphenylphosphino)ethane ligand, which favors for steric reasons in **2b** effective crystallization of a single enantiomeric form over that of a racemic mixture. The excessive steric hindrance in **2b** is reflected in relevant geometric

Table 2
Selected geometric parameters

Compound	**2a**[a]	**2b**	**2c**
(i) Torsion angles between adjacent pyrrole rings (°)			
'a'–'b'	47.2(3), 44.1(4)	46.9(3)	45.8(1)
'b'–'c'	23.1(4), 24.7(4)	17.8(4)	22.1(1)
'c'–'d'	5.8(5), 8.7(5)	0.7(5)	5.8(1)
'd'–'a'	16.1(4), 16.7(3)	29.5(3)	28.5(1)
(ii) Deviations of the $(C{=}O)_{organic}$, N_a, N_b, and Rh atoms from the mean plane of rings 'c' and 'd' (Å)			
C (C=O)	−0.49(1), −0.52(1)	−0.426(7)	−0.461(4)
O (C=O)	−1.10(1), −1.12(1)	−1.095(7)	−1.100(4)
N_a	1.06(1), 1.00(1)	0.903(9)	0.993(5)
N_b	1.07(1), 1.04(1)	1.004(10)	0.998(5)
Rh	2.194(8), 2.185(7)	2.340(6)	2.280(3)
(iii) Coordination distances of Rh to it nearest neighboring atoms N_a, N_b, L, and L′ (Å) (L and L′ represent the inorganic carbonyl carbon in **2a**, the P-atoms in **2b**, and C-atoms of the C=C double bonds of the 'cod' ligand in **2c**)			
N_a	2.055(6), 2.064(7)	2.104(5)	2.066(3)
N_b	2.032(7), 2.039(7)	2.094(5)	2.070(3)
L	1.850(10), 1.894(12)	2.210(2)	2.152–2.154(5)
L′	1.860(10), 1.866(10)	2.209(2)	2.132–2.153(5)

[a] **2a** contains two crystallographically independent corrole molecules in the asymmetric unit.

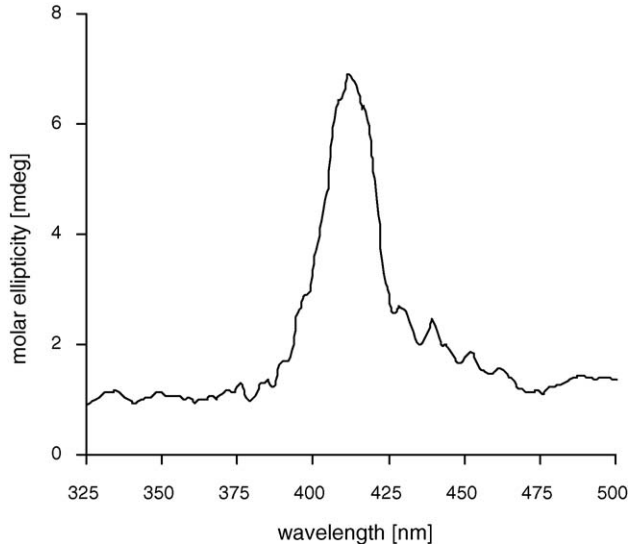

Fig. 5. CD spectrum of complex **2b** after spontaneous resolution by recrystallization.

parameters in this structure (Table 2), including significantly longer Rh–N(pyrrole) bond distances and a much wider distortion of the rhodium atom along with its immediate coordination environment (the square-planar fragment defined by Rh, N_a, N_b, and the P atoms) from the plane of the corrole macrocycle. Importantly, examination of the bulk material obtained from crystallization of complex **2b** by circular dichroism (Fig. 5) revealed a strong signal indicative of the spontaneous resolution.

4. Conclusions

This study describes facile procedures for insertion of rhodium into an easily accessible chiral corrole, leading to rhodium(I) complexes of the new chiral corrole. The diamagnetic ring current effect of the corroles allows for quite straightforward and detailed analysis of the structural aspects by solution state NMR and these conclusions were further corroborated by X-ray crystallography. These findings will be used in future studies that will be devoted to utilization of these complexes as catalysts for asymmetric processes.

5. Supplementary material

Crystallographic data of the structural analyses have been deposited with the Cambridge Crystallographic Data Center, CCDC Nos. 289475, 289476, and 289477 for structures **2a**, **2b**, and **2c**, respectively. Copies of this information may be obtained free of charge from The Director, CCDC, 12 Union Road, Cambridge CB2 1EZ, UK (fax: +44 1223 336 033; e-mail: deposit@ccdc.cam.ac.uk or website: http://www.ccdc.cam.ac.uk).

Acknowledgements

This research was supported by the German Israeli Project (DIP, ZG) and the Israel Science Foundation under Grant 254/04 (IG). Funding of IS by the Center for Absorption in Science – Ministry of Immigration – is acknowledged.

References

[1] (a) For review that cover the recently introduced synthetic methodologies, see: D.T. Gryko, Eur. J. Org. Chem. (2002) 1735;
(b) J.P. Collman, R.A. Decreau, Tetrahedron Lett. 44 (2003) 1207;
(c) D.T. Gryko, B. Koszarna, Org. Biomol. Chem. 1 (2003) 350;
(d) R.A. Decrĕau, J.P. Collman, Tetrahedron Lett. 44 (2003) 3323.
[2] (a) Z. Gross, L. Simkhovich, N. Galili, J. Chem. Soc., Chem. Commun. (1999) 599;
(b) A. Mahammed, H.B. Gray, A.E. Meier-Callahan, Z. Gross, J. Am. Chem. Soc. 125 (2003) 1162.
[3] J. Grodkowski, P. Neta, E. Fujita, A. Mahammed, Z. Gross, J. Phys. Chem. A 106 (2002) 4772.
[4] (a) Z. Gross, G. Golubkov, L. Simkhovich, Angew. Chem. Int. Ed. Engl. 39 (2000) 4045;
(b) G. Golubkov, J. Bendix, H.B. Gray, A. Mahammed, I. Goldberg, A.J. DiBilio, Z. Gross, Angew. Chem. Int. Ed. Engl. 40 (2001) 2132;
(c) R.A. Eikey, S.I. Khan, M.M. Abu-Omar, Angew. Chem. Int. Ed. Engl. 41 (2002) 3592;
(d) H.-Y. Liu, T.-S. Lai, L.-L. Yeung, C.K. Chang, Org. Lett. 5 (2003) 617;
(e) J.P. Collman, L. Zeng, R.A. Decrĕau, Chem. Commun. (2003) 2974.
[5] L. Simkhovich, Z. Gross, Tetrahedron Lett. 42 (2001) 8089.
[6] (a) L. Simkhovich, A. Mahammed, I. Goldberg, Z. Gross, Chem. Eur. J. 7 (2001) 1041;
(b) L. Simkhovich, I. Goldberg, Z. Gross, J. Porphyrins Phthalocyanines 6 (2002) 439.
[7] (a) L. Simkhovich, N. Galili, I. Saltsman, I. Goldberg, Z. Gross, Inorg. Chem. 39 (2000) 2704;
(b) J.P. Collman, H.J.H. Wang, R.A. Decreau, T.A. Eberspacher, C.J. Sunderland, Chem. Commun. (2005) 2497.
[8] (a) Z. Gross, N. Galili, I. Saltsman, Angew. Chem. Int. Ed. Engl. 38 (1999) 1427;
(b) Z. Gross, N. Galili, L. Simkhovich, I. Saltsman, M. Botoshansky, D. Bläser, R. Boese, I. Goldberg, Org. Lett. 1 (1999) 599.
[9] I. Saltsman, I. Goldberg, Z. Gross, Tetrahedron Lett. 44 (2003) 5669.

[10] I. Saltsman, L. Simkhovich, Y. Balazs, I. Goldberg, Z. Gross, Inorg. Chim. Acta 357 (2004) 3038.
[11] A. Altomare, M.C. Burla, M. Camalli, M. Cascarano, C. Giacovazzo, A. Guagliardi, G. Polidori, SIR-92/97, J. Appl. Crystallogr. 27 (1994) 435.
[12] P.T. Beurskens, G. Admiraal, G. Beurskens, W.P. Bosman, S. Garcia-Granda, R.O. Gould, J.M.M. Smits, C. Smykalla, The DIRDIF-96 Program System, Technical Report of the Crystallography Laboratory, University of Nijmegen, The Netherlands, 1996.
[13] G.M. Sheldrick, SHELXL-97, Program for the Refinement of Crystal Structures from Diffraction Data, University of Göttingen, Germany, 1997.
[14] C. Brown, B.T. Heaton, L. Longhetti, W.T. Povey, D.O. Smith, J. Organomet. Chem. 192 (1980) 93.